

# EXAFS Debye-Waller factors issued from Car-Parrinello molecular dynamics: Application to the fit of oxaliplatin and derivatives

K. Provost,<sup>1,a)</sup> E. C. Beret,<sup>2</sup> D. Bouvet Muller,<sup>1</sup> A. Michalowicz,<sup>1</sup> and E. Sánchez Marcos<sup>2</sup>

<sup>1</sup>ICMPE, UMR 7182 CNRS, UPEC, PRES Paris Est, Thiais 94320, France

<sup>2</sup>Departamento de Química Física, Universidad de Sevilla, Sevilla 41012, Spain

(Received 20 November 2012; accepted 23 January 2013; published online 25 February 2013)

One of the main pitfalls in EXAFS fitting is correlation among parameters, which can lead to unreliable fits. The use of theoretical Debye-Waller factors (DWs) is a promising way to reduce the number of fitted parameters. When working with molecular dynamics, it is not only possible to evaluate DWs from the statistical distributions issued from the trajectory but also to estimate the distribution anharmonicity, and to compute simulated average EXAFS spectra that can be fitted as experimental ones, in order to assess the ability of EXAFS fitting to recover information on DWs, as well as other structural and spectroscopical parameters. The case studied is oxaliplatin, a third generation anticancer drug. The structural information and the simulated average spectra were derived from a Car-Parrinello molecular dynamics (CP-MD) trajectory of a compound closely related to oxaliplatin. We present the DWs issued from this simulation and their use, by taking their theoretical absolute values (no DW fitted) or their ratios (one DW fitted). In this second approach, the fit of oxaliplatin experimental spectra leads to DWs values very close to the theoretical ones. This shows that the CP-MD trajectory provides a good representation of the distance distributions for oxaliplatin. Transferability of oxaliplatin DWs, for all relevant single and multiple scattering paths, to closely related compounds is proven for the case of bis(oxalato)platinum(II) and bis(ethylene diamine)platinum(II).  
 © 2013 American Institute of Physics. [<http://dx.doi.org/10.1063/1.4790516>]

## I. INTRODUCTION

Fitting EXAFS spectra has become an extremely useful tool to solve the local structure around an absorbing atom for many chemical systems in all matter states. Its main capability concerns systems lacking a long-range order and the technique has proved to be particularly efficient to characterize disordered coordination spheres. Structure determination by EXAFS is usually based on the standard EXAFS equation (1) proposed by Sayers, Stern and Lytle,<sup>1</sup> and the fit of different structural parameters (distances  $R_i$  and Debye-Waller factors  $\sigma_i$ , in the assumption of harmonic distance distributions) for a given model (set of relevant scattering paths  $i$ , with  $N_i$  equivalent scattering paths of effective amplitude  $|f_i(k, R_i)|$  and phase  $\psi_i(k)$ ),<sup>2</sup>

$$k\chi(k) = s_0^2 \sum_i \frac{N_i}{R_i^2} |f_i(k, R_i)| e^{-2\sigma_i^2 k^2} e^{-2R_i/\lambda(k)} \times \sin(2kR_i + 2\delta_1(k) + \psi_i(k)). \quad (1)$$

A long recognized shortcoming in EXAFS fitting comes from correlations among parameters, in particular those affecting the amplitude: electronic reduction factor  $s_0^2$ , number of equivalent paths  $N_i$ , effective scattering amplitude  $|f_i(k, R_i)|$ , Debye-Waller factor (DW)  $\sigma_i$ , and mean free path  $\lambda(k)$ . When scattering paths with similar effective amplitudes and phases have different distances, interference effects may in-

duce strong correlations between distance and amplitude parameters. Then, the fitting of a large number of DWs may lead to wrong structural solutions.<sup>3</sup>

In order to deal with a small number of independent DWs, different authors have proposed the use of XAS-external information, which has been either experimental<sup>4</sup> or theoretical. Thus, on the basis of geometrical relationships and statistical uncertainties, Yokoyama *et al.*<sup>5</sup> proposed fixed values for ratios among the different DWs of related single and multiple scattering paths. Several authors have undertaken DW estimations based on the vibrational properties of the ensemble of neighbor atoms surrounding the absorber atom.<sup>6</sup> Another way for undertaking the theoretical estimation of DWs is based on the use of statistical structural distributions provided by computer simulations. Filipponi *et al.* include implicitly the DWs in the fit by means of structural correlation functions.<sup>7</sup> Another strategy is the explicit computation of cumulants of the corresponding geometrical paths.<sup>8-10</sup> Theoretical DW values have also been used in approaches where quantum-mechanical optimization and EXAFS fitting are coupled.<sup>11</sup> However, to our knowledge, no systematic evaluation of the impact of such theoretical DWs on EXAFS fitting has been done.

For such an evaluation, the main difficulty comes from the fact that other amplitude parameters are not always well controlled, when dealing with experimental spectra, with different ways of computing phases and amplitudes<sup>12,13</sup> or inelastic loss parameters.<sup>13,14</sup> These amplitude parameters may be a source of systematic errors in the fitting procedure when working on experimental spectra.

<sup>a)</sup> Author to whom correspondence should be addressed. Electronic mail: provost@u-pec.fr.

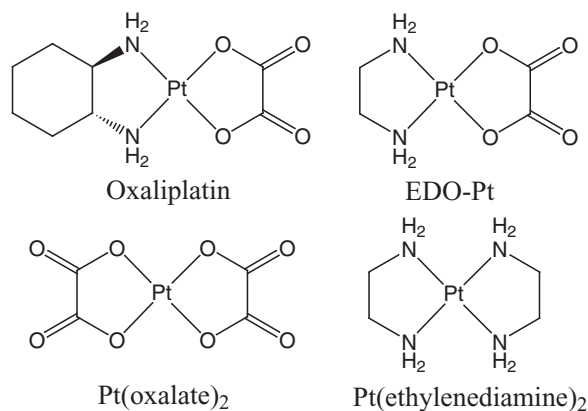


FIG. 1. Oxaliplatin, EDO-Pt, bis(oxalato)platinum(II), and bis(ethylenediamine)platinum(II) structures

EXAFS spectra, simulated from a molecular dynamics (MD) trajectory, implicitly account for a statistical representation of the structure and its fluctuations, including anharmonicity behaviors. Then, uncertainties related to effective amplitudes, inelastic loss parameters, and the electronic reduction factor can be minimized, and a thorough analysis of the impact of DWs can be easily monitored. In this way, the fitting of simulated spectrum provides a well-controlled information to develop new fitting strategies in EXAFS and to assess their physical consistencies.

This approach is applied to oxaliplatin, a third generation anticancer drug of the cisplatin family.<sup>15</sup> Oxaliplatin contains a Pt(II) square planar coordinated by two bidentate ligands: oxalate and diaminocyclohexane (Fig. 1). Its main pharmaceutical interest comes from the diaminocyclohexane ligand,<sup>16</sup> which is generally considered as inert.<sup>17,18</sup> The EXAFS spectrum of oxaliplatin as well as of several parent drugs and their degradation products have been previously recorded and analyzed by some of our group.<sup>19</sup> In addition, we performed a Car-Parrinello molecular dynamics (CP-MD) simulation of ethyldiamineoxalatoplatinum(II) (EDO-Pt), a model structure for oxaliplatin obtained by removal of the outer part of the cyclohexane ring (Fig. 1), in water.<sup>20</sup> Chemical studies suggest that the cutting of the external part of diaminocyclohexane does not affect the complex reactivity.<sup>17</sup> The comparison of theoretical XANES and EXAFS spectra calculated either using a unique structure of oxaliplatin or EDO-Pt, or averaging on a significant number of structures extracted from the EDO-Pt trajectory, showed that EDO-Pt is a good spectroscopical model for oxaliplatin.<sup>21</sup> The systematic errors, associated with the distances determination in a standard EXAFS fitting approach, were assessed by fitting both the simulated and experimental spectra under the same conditions.

In this work, we extend our first study<sup>21</sup> to the extraction of information on DWs from the CP-MD trajectory and their use in new approaches for accurate constrained EXAFS fitting. For both single scattering and multiple scattering paths, analysis of the distance distributions is used to support the DWs estimation on the basis of the second cumulant, as proposed by Merklings *et al.*<sup>10</sup> Then they are used either through their absolute values coming from the simulation or some of their ratios. In the last case, an empirical DW  $\sigma_1^2$  will be fit-

ted for the first coordination sphere single scattering paths, and the rest of DWs are derived from  $\sigma_1^2$  by applying ratios based on the MD values according to the following equation:

$$\sigma_i^2 = \frac{(\sigma_i^2)^{MD}}{(\sigma_1^2)^{MD}} \sigma_1^2. \quad (2)$$

In this way, the degree of transferability of theoretical ratios to the experimental ones can be explored.

This paper deals with the use of MD DWs ratios (**MDR**) or values (**MDV**) for the fit of experimental EXAFS spectra of oxaliplatin. The comparison of these two DWs approaches with other strategies on DWs constraints will be described elsewhere. A step beyond is the transferability of these ratios to other structurally related compounds, such that an enhancement of their fitting could be achieved. The question has been addressed, in this work, by undertaking the EXAFS fitting of two compounds closely related to oxaliplatin, whose come from the substitution of one of the platinum(II) bidentate ligands to get the symmetric complexes: bis(oxalato) platinum(II) and bis(ethylenediamine)platinum(II) (Fig. 1).

## II. METHODOLOGY

### A. Simulated spectra and MD-based Debye-Waller factors

Simulated Pt L<sub>III</sub>-edge EXAFS spectra of oxaliplatin have been computed using a statistically meaningful number of snapshots ( $N_{MD}$ ) extracted from the CP-MD simulation of EDO-Pt in aqueous solution as described in Ref. 20 (The system was formed by 1 EDO-Pt molecule plus 63 water molecules. The simulation time was 32 ps—6 ps for thermalization and 26 ps for production—which needed around 400 h of computer time using 90 processors). For each snapshot  $M$ , an individual spectra  $\chi_M(k)$  is computed, and the  $N_{MD}$  resulting spectra are averaged to yield the simulated EXAFS spectrum  $\bar{\chi}(k)$ :

$$\bar{\chi}(k) = \frac{1}{N_{MD}} \sum_M \chi_M(k). \quad (3)$$

The average EXAFS signal is obtained by the following equation:<sup>9,10</sup>

$$\bar{\chi}(k) = \frac{1}{N_{MD}} \sum_M \sum_i^{paths} \frac{N_i s_0^2 |f_{eff}(k, R)|_i}{k R_{Mi}^2} e^{-2R_{Mi}/\lambda} \times \sin(2k R_{Mi} + \alpha_{Mi}(k)), \quad (4)$$

where index  $i$  denotes a given scattering path. It is worth noting that Eq. (4) differs from the conventional EXAFS equation (1)<sup>1</sup> in the fact that the exponential factor containing the DW has been replaced by a sum over a high number of MD structural arrangements (snapshots) which account for the thermal and structural disorder. This change has fundamental implications because the need of a model or a reference structure disappears when a simulated spectrum is computed.<sup>22</sup> In this study, a  $N_{MD}$  value of 250 has been used. Snapshots were extracted from the CP-MD simulation of EDO-Pt in water already published. A higher number of

snapshots (500) was used to check that no observable changes appear into the simulated spectrum.

EXAFS calculations were performed with the FEFF8 code (version 8.4).<sup>23</sup> The Hedin-Lundqvist exchange-correlation potential was used to compute the electron density distribution within a self-consistent-field (SCF) approach. Hydrogen atoms were included in the SCF procedure to compute the potential, but they were not included as backscatters. In the simulated EXAFS spectra, the only parameter not derived from computation was the amplitude reduction function,  $s_0^2$ , that was set up to 0.94 in order to match the first peak height of the experimental and simulated Fourier transform (FT) of EXAFS spectra. A similar strategy to obtain simulated EXAFS and XANES spectra of different ions in solution has been successfully applied in previous works.<sup>9,10,22,24</sup> In this work, the solvation structure has not been included, neither in the computation of simulated spectra nor in the fitting procedure, because its contribution is really small to the EXAFS function. (CP-MD simulations show that the first shell of water molecules is at a 4.14 Å distance from platinum<sup>20,21</sup>; refer also to Sec. II C).

The MD-based Debye-Waller factors were computed on the basis of the distribution of intramolecular distances, as proposed by several authors:<sup>8,9</sup>

$$\sigma_i^2 = \langle (\bar{R}_i - R_i)^2 \rangle \quad (5)$$

To this aim, a large number of snapshots (ca. 25 000) were used. The calculation of DWs on the sole basis of the second cumulant is well supported by Gaussian-like distributions of distances in EDO-Pt, as shown in Sec. III A.

## B. Experimental spectra

Oxaliplatin was obtained from different Sanofi pharmaceutical preparations: powder (excipient monohydrate lactose; OxaliPt-sol, OxaliPt-liq1), used to prepare pellets or diluted in pure water to get a 10 mg/ml (25 mM) solution, or solution 5 mg/ml ready for injection (solvent: water, no excipient; OxaliPt-liq2, OxaliPt-liq3). In these aqueous solutions, oxaliplatin is known to be very stable. Potassium bis(oxalato) platinate(II) and bis(ethylenediamine) platinum(II) chloride were purchased from Sigma Aldrich and prepared as pellets. For all samples, the total absorbance after edge was less than 1.0, with an absorbance jump of 0.5 for solids and 0.1–0.15 for liquids. Pt-L<sub>III</sub>-edge XAS spectra were recorded in transmission mode during different runs, at LURE (Orsay, France, EXAFS13 station of the DCI storage ring, Si(111) double crystal monochromator, resolution  $\Delta E/E > 2 \times 10^{-4}$ ) for the solid (OxaliPt-sol), and at ELETTRA (Trieste, Italy, BL11.1 station, Si(111) double crystal monochromator, resolution  $\Delta E/E \sim 10^{-4}$ ; OxaliPt-liq1), ESRF (Grenoble, France, BM29 station, Si(311) double crystal monochromator, resolution  $\Delta E/E \sim 1.5 \times 10^{-4}$ ; OxaliPt-liq2), and SOLEIL (Saint Aubin, France, SAMBA station, Si(111) double crystal monochromator, resolution  $1.7 \Delta E/E \sim 10^{-4}$ ; OxaliPt-liq3) for liquids, with an energy-range of 11 260–13 000 eV. Harmonic rejection was achieved with a total reflection mirror at Elettra and SOLEIL, using a slight detuning of the double crystal monochromator at LURE (the flux at the third har-

monic was very low) and a 50% detuning of both crystals at ESRF. All spectra were recorded at room temperature.

The spectra were extracted using standard procedures<sup>13,25</sup> available in the program Cherokee (MAX),<sup>26</sup> including spline smoothing atomic absorption determination, energy-dependent normalization and fast Fourier transform ( $E_0$  taken at the inflection point 11568 eV, FT range 2.3–16 Å<sup>-1</sup>). Each spectrum was recorded three times in order to estimate the average and the experimental errors. The noise was suppressed by filtering all signals above 5 Å.

## C. Fitting procedure

Both simulated and experimental spectra were fitted using the same procedure. The fits were performed on the 2.3–16.0 Å<sup>-1</sup>  $k$ -range with a  $k^3$ -weighting. Effective phases and amplitudes were calculated with FEFF8<sup>23</sup> on the basis of the different model structures: the EDO-Pt gas-phase structure<sup>20</sup> optimized quantum-mechanically, and, the oxaliplatin, bis(oxalato) platinate(II), and bis(ethylenediamine) platinum(II) crystallographic structures.<sup>27,28</sup> The backscattering potentials were derived either from a SCF electronic density of the system (SCF) or using the atomic tabulated data (noSCF). All fits use FEFF8 mean free paths, except for some of the fits presented in Table IV(b), where the empirical minimal curve ( $\Gamma = 0.7$ ,  $\eta = 3.0$ ) was applied.<sup>13</sup> The introduction of a second mean free path model at this step of the study aimed to check that our results were not influenced by the choice of the mean free path model. Finally,  $s_0^2$  was fitted.

The fitting procedure includes two steps:

- (1) Fit of the first coordination sphere, on the basis of a 4 Pt-(N/O) shell: In this step, first coordination sphere filtered spectra (0–2.2 Å range) are used. The energy correction  $\Delta E$ , a unique distance  $R$ ,  $s_0^2$ , and a unique DW ( $\sigma^2$ ) are fitted.
- (2) Fitting of the whole signal on the basis of a 7-shell model previously tested on oxaliplatin:<sup>21</sup> single scattering (SS) paths in the first coordination sphere (paths **1a** and **1b** considered as a unique contribution **1**, see Fig. 2); SS paths in the second coordination sphere (**2–3**); main SS and multiple scattering (MS) paths of oxalate (**4–6**); MS through platinum (**7**). Path selection was done according to the paths amplitudes in the fitting  $k$ -range. The amplitude of the 3-legs Pt-N-O scattering path (**8**) is much lower than that of the 4-legs scattering path involving the same atoms (**7**) one in the 2.3–16 Å<sup>-1</sup>  $k$ -range with a  $k^3$ -weighting. The remaining scattering paths have low contributions to the EXAFS signal. In our previous study,<sup>21</sup> we have shown that the solvation structure could hardly be detected, only on the simulated spectrum, at a distance of 4.14 Å from platinum. The solvent contribution is too low to be detected on our experimental structures. A new set of experimental data for oxaliplatin in solid and solution recorded on the same beamline under equivalent conditions should be carried out to undertake this question. Thus the water molecules are neglected in this study. In the second step,  $\Delta E$  is set to the value extracted from the first step.

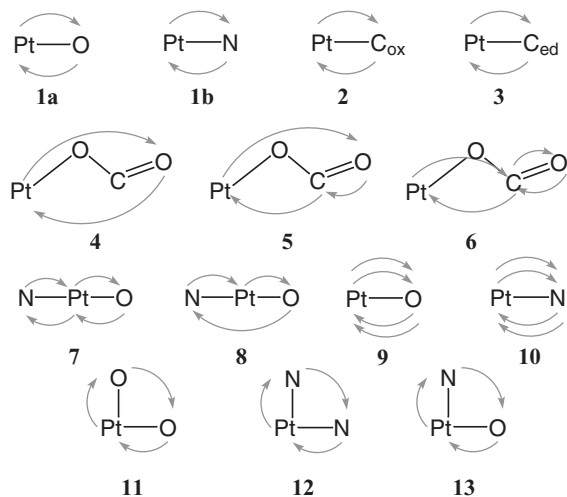


FIG. 2. Scattering path numbering.  $C_{ox}$  and  $C_{ed}$  are the carbon atoms belonging to the oxalate and ethylenediamine ligands, respectively. EXAFS fits include signals for paths 1–7 only.

Due to implicit correlations among the different paths, in this second step, constraints were applied on distances, in order to limit the number of fitted distances to 3. For EDO-Pt, oxaliplatin and bis(oxalato) platinate(II), a common distance is employed for scattering paths 4–5–6 of oxalate ( $R_4 = R_5 = R_6$ ), and a distance shift of  $\Delta R_{47} = R_7 - R_4 = 0.1 \text{ \AA}$  is applied between oxalate scattering paths and MS through platinum 7. For EDO-Pt and oxaliplatin, a second distance shift of  $\Delta R_{23} = R_3 - R_2 = 0.1 \text{ \AA}$  is used, between the two Pt-C SS paths. These distance shifts values are based on EDO-Pt optimized structure ( $\Delta R_{23} = 0.14 \text{ \AA}$  and  $\Delta R_{47} = 0.11 \text{ \AA}$ )<sup>20</sup> and oxaliplatin crystallographic structure ( $\Delta R_{23} = 0.13 \text{ \AA}$  and  $\Delta R_{47} = 0.07 \text{ \AA}$ ).<sup>27</sup>

CP-MD based DWs for EXAFS fitting have been tested adopting two strategies (**MDR** and **MDV** options), which introduce a different DW for each scattering path. In the **MDV** case (MD Values), the DW values are obtained from the MD trajectory according to Eq. (5) and fixed, i.e., none of the DWs are fitted. The second strategy consists in fitting the DW for SS within the first coordination sphere ( $\sigma_1^2$ ), whereas the rest of DWs are obtained from  $\sigma_1^2$  according to the ratios observed between the MD-DWs as expressed in Eq. (2). This option is called **MDR** (MD ratios).

All the fits were performed using the RoundMidnight code.<sup>26</sup> The statistical errors ( $\epsilon_i$ ) on the average spectra and error bars for the fitted parameters were evaluated as recommended by the IXS Standard and Criteria Subcommittee.<sup>29</sup> According to these recommendations, the goodness of fit or quality factor is  $QF = \Delta\chi_{\min}^2/\nu$ , where  $\Delta\chi_{\min}^2$  is the minimum value of the statistical  $\Delta\chi^2$  and  $\nu = N_{ind} - N_{par}$  is the degree of freedom.  $N_{ind}$  is the number of independent points and  $N_{par}$  is the total number of fitted parameters. Since a  $k^3$ -weighting is used, the statistical  $\Delta\chi^2$  in  $k$ -space is calculated as proposed by Vlais *et al.*<sup>30</sup> In  $R$ -space,  $\Delta\chi^2$  is calculated according to Ref. 29. The mean experimental error ( $\epsilon$ ) is calculated on  $k\chi_{exp}$  spectra by evaluating the point dispersion, corrected by the Student statistics as recommended by the IXS Standard and Criteria Subcommittee. In the fitting range,  $\langle\epsilon\rangle$

ranges between 0.011 and 0.027 for the experimental spectra. For theoretical spectra, an error of the same order of magnitude as for the experimental spectra:  $\langle\epsilon\rangle = 0.015 \text{ \AA}$  was adopted.

### III. RESULTS AND DISCUSSION

#### A. MD-based DW factors

Figure 3 shows the distance distributions (red lines) for scattering paths 1–7, obtained from the CP-MD trajectory. These distributions are nicely fitted by Gaussian functions (black lines in Fig. 3), which supports the DW computation as the second-order cumulant of an EDO-Pt scattering paths. As long as we consider the sole EDO-Pt molecular structure, no clear anharmonicity is observed. This is not the case for scattering paths involving hydration water molecules.<sup>20</sup> Such a Gaussian behavior of intramolecular distances in EDO-Pt is due to the strong bonding interactions between the Pt cation and its ligands, what was already observed in the analysis of the radial distribution functions for this compound.<sup>20</sup>

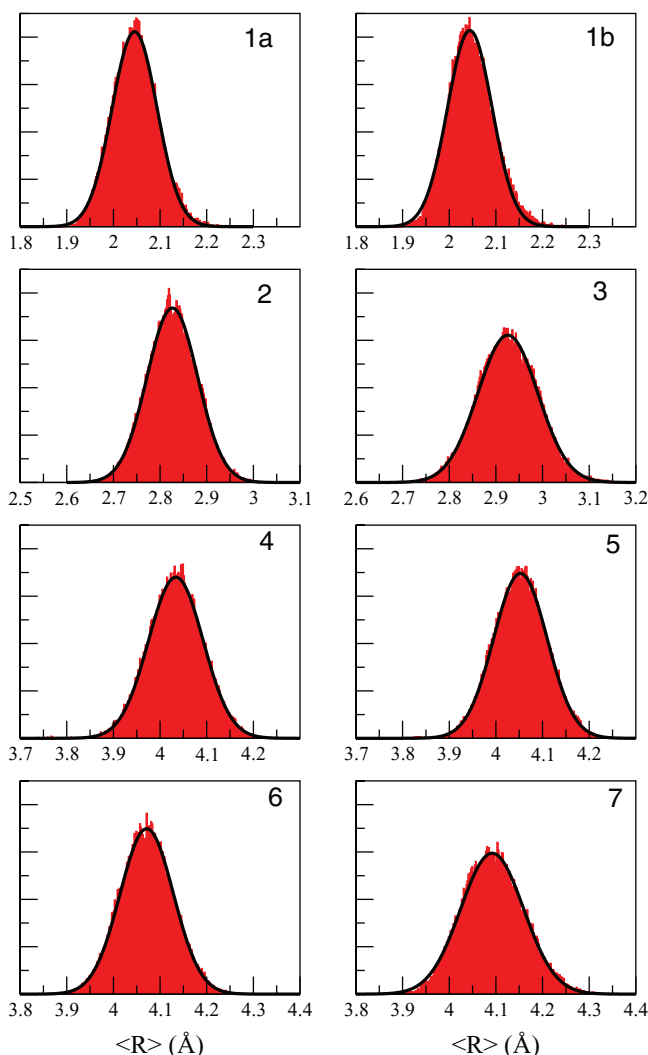


FIG. 3. Distance distributions of the scattering paths 1–7 (red) and their fits by a Gaussian function (black line).

TABLE I. Average distances ( $\bar{R}_{CP-MD}$ ) and MD-based DW factors ( $\sigma_{CP-MD}^2$ ).  $N_{leg}$  is the number of legs of each path.

Path <sup>a</sup>	$N_{leg}$	$\bar{R}_{CP-MD}$ (Å)	$\sigma_{CP-MD}^2$ (Å <sup>2</sup> )	Path	$N_{leg}$	$\bar{R}_{CP-MD}$ (Å)	$\sigma_{CP-MD}^2$ (Å <sup>2</sup> )
<b>1a</b>	2	2.047	0.0024	<b>1b</b>	2	2.048	0.0024
<b>2</b>	2	2.826	0.0029	<b>3</b>	2	2.925	0.0041
<b>4</b>	2	4.032	0.0035	<b>5</b>	3	4.052	0.0033
<b>6</b>	4	4.071	0.0032	<b>7</b>	4	4.094	0.0044
<b>8</b>	3	4.091	0.0044	<b>9</b>	4	4.094	0.0095
<b>10</b>	4	4.095	0.0098	<b>11</b>	3	3.385	0.0029
<b>12</b>	3	3.409	0.0039	<b>13</b>	3	3.585	0.0062

<sup>a</sup>For the path index, refer to Fig. 2.

Table I presents the average distances and DWs, computed from the CP-MD simulation, for the scattering paths defined in Fig. 2. Despite the different nature of the two bidentate ligands, oxalate and ethyldiamine, the two single scattering (SS) paths within the first coordination sphere (**1a**: Pt-O and **1b**: Pt-N) present almost the same average distance as well as distance distribution. Distances obtained for the two Pt-C SS paths (**2–3**) differ by 0.1 Å ( $R_{Pt-C_{ed}} - R_{Pt-C_{ox}}$ ). This was already observed in the model structures, EDO-Pt quantum-mechanically optimized<sup>20</sup> and oxaliplatin crystallographic data.<sup>27</sup> Furthermore, Pt-C<sub>ed</sub> distance distribution (**3** in Fig. 3) is much broader than the Pt-C<sub>ox</sub> one (**2** in Fig. 3), ( $\sigma_3^{MD}$  being 30% larger than  $\sigma_2^{MD}$  value).

At first sight, it could be expected a good correlation between the DW values and their corresponding path lengths: the DW values for SS in the first coordination sphere ( $R \sim 2$  Å) should be the smallest ones, then DWs for SS in the second coordination sphere ( $R \sim 3$  Å) should be somewhat larger, followed by the triangular scattering paths ( $R \sim 3.5$  Å), whereas the largest DWs values would correspond to paths with length around 4 Å [oxalate SS and multiple scattering (MS), and MS through Pt]. However, this is not the behavior observed in Table I. The different degree of flexibility of oxalate and ethylenediamine ligand is responsible for a different sequence of values. Pt-C<sub>ed</sub> (**3**) DW appears to be closer to Pt-N-Pt-O MS DW (**7**) than to that of Pt-C<sub>ox</sub> (**2**), while DWs associated with oxalate scattering (**4–6**) are closer to Pt-C<sub>ox</sub> DW than to Pt-N-Pt-O DW. In fact, the average DW for all Pt-C scattering paths (both Pt-C<sub>ox</sub> and Pt-C<sub>ed</sub> paths:  $\sigma_{Pt-C_{ox/ed}}^2 = 0.0035$  Å<sup>2</sup>) is still slightly larger than the average DW factor of all oxalate paths (paths **4–5–6**:  $\sigma_{ox}^2 = 0.0033$  Å<sup>2</sup>).

In the 1st coordination sphere, DWs for MS through platinum (**7–8**) are almost twice those of SS DWs (**1a–1b**). In addition, ratios between Pt-O-Pt-O (**9**) and Pt-O(**1a**) on one hand, and Pt-N-Pt-N (**10**) and Pt-N (**1b**) on the other hand, are close to 4. Such ratios agree with Yokoyama's model for 1st coordination sphere MS DW factors.<sup>5</sup> However, Yokoyama's empirical ratios for triangular paths cannot be applied to the system under study: the DW values obtained for the triangular paths are rather different for Pt-O-O (**11**) ( $\sigma_{PtOO}^2 = 0.0029$  Å<sup>2</sup>), Pt-N-N (**12**) ( $\sigma_{PtNN}^2 = 0.0039$  Å<sup>2</sup>) and Pt-N-O (**13**) ( $\sigma_{PtNO}^2 = 0.0062$  Å<sup>2</sup>). The values of paths **11** and **12** are respectively close to the Pt-C<sub>ox</sub> (**2**) and Pt-C<sub>ed</sub> (**3**) ones, whereas the Pt-N-O (**13**) DW is twice that of the Pt-O-O one.

Thus the assignment of empirical ratios for triangular paths should be done with a special care, particularly in the case of bidentate ligands. For such scattering paths or for more complex systems, the use of ratios derived from theoretical approaches appears to be a more reliable strategy than the use of empirical ones.

## B. Fit of EDO-Pt simulated and oxaliplatin experimental spectra

Figure 4 presents EDO-Pt simulated spectrum and the different oxaliplatin experimental spectra recorded on liquid and solid samples. Since this paper deals with the question of DWs in EXAFS, an aim is to check to which point the theoretical values can be validated by experiment, using oxaliplatin experimental spectra. A first step is to check that EXAFS fit

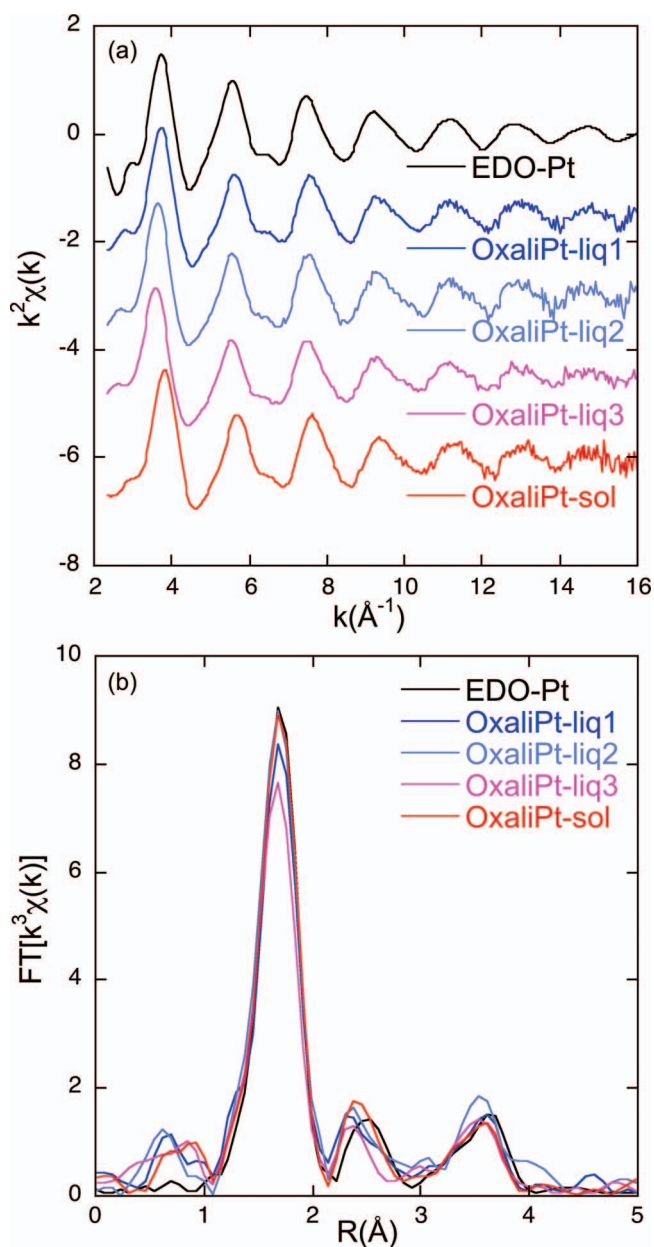


FIG. 4. EDO-Pt simulated and oxaliplatin experimental spectra (a) and their Fourier transform modulus (b).

TABLE II. EXAFS fit of EDO-Pt.<sup>a</sup>

	noSCF		SCF		CP-MD
	MDR	MDV	MDR	MDV	
$s_0^2$	1.24(7)	1.10(5)	0.95(3)	0.92(2)	
$\sigma_1^2 \times 10^4$ <sup>b</sup>	36(5)	24	26(3)	24	24
$R_1$	2.02(1)	2.02(1)	2.03(1)	2.03(1)	2.05(5)
$R_2$	2.80(2)	2.80(2)	2.86(1)	2.86(1)	2.83(5)
$R_4$	3.99(2)	4.00(2)	4.07(1)	4.07(1)	4.05(8)
QF	1.93	2.23	0.65	0.65	

<sup>a</sup>Error ( $\epsilon$ ) = 0.015.<sup>b</sup> $\sigma_1^2$  values expressed in  $\text{\AA}^2$ , distances expressed in  $\text{\AA}$ . Other distances derived from  $R_2$  and  $R_4$  using constraints described in Sec. II C.

of simulated spectra provides DW values close to theoretical ones, before extracting information on DWs from experimental spectra, in a second step. However, experimental EXAFS data may be perturbed by systematic errors, in particular those related to the extraction procedure. This is the reason why we include in this study different experimental spectra, recorded in different synchrotron sources and independently studied, to have an estimation of the error related to the extraction procedure. Figure 4(b) shows that, despite a careful sample preparation and spectra extraction, non-negligible changes can be observed in the Fourier transform main peak amplitude, which may impact the fitted amplitude parameters.

Simulated spectra were generated using SCF based phases and amplitudes. However, most EXAFS studies are performed with **noSCF** phases and amplitudes. For this reason, we tested **MDR** and **MDV** for both **SCF** and **noSCF** phases and amplitudes, in order to check whether a refined model of scattering potentials was necessary or not, in the purpose of including CP-MD DWs in EXAFS fits.

For all spectra, good fits are obtained when using either **MDR** or **MDV** whatever the choice applied for the determination of the effective scattering amplitudes (**noSCF** or **SCF**). The quality factors are close to 1 or lower, and the fitted distances are in good agreement with the actual distances which are average distances issued from the CP-MD trajectory for EDO-Pt,<sup>20</sup> or the crystallographic structure for oxaliplatin.<sup>27</sup> Tables II and III present the fitted parameters obtained re-

TABLE III. EXAFS fit of OxaliPt-liq1.<sup>a</sup>

	noSCF		SCF		Cryst.
	MDR	MDV	MDR	MDV	
$s_0^2$	1.07(7)	0.99(4)	0.80(5)	0.82(3)	
$\sigma_1^2 \times 10^4$ <sup>b</sup>	32(4)	24	22(4)	24	
$R_1$	2.00(1)	2.00(1)	2.02(1)	2.02(1)	2.04(2)
$R_2$	2.76(2)	2.76(2)	2.85(2)	2.85(2)	2.77(7)
$R_4$	3.97(2)	3.98(2)	4.04(2)	4.04(2)	4.00(2)
QF	1.54	1.64	1.35	1.32	

<sup>a</sup>Experimental error ( $\epsilon$ ) = 0.015.<sup>b</sup> $\sigma_1^2$  values expressed in  $\text{\AA}^2$ , distances expressed in  $\text{\AA}$ . Other distances derived from  $R_2$  and  $R_4$  using constraints described in Sec. II C.

spectively for EDO-Pt simulated spectrum and one of the experimental spectra (OxaliPt-liq1, 10 mg/ml solution, excipient, Elettra; for other samples, see supplementary material<sup>31</sup>). Figure 5 displays the corresponding experimental and theoretical EXAFS signals. When using SCF based phases and amplitudes, the distances are slightly improved. However, the quality factor reduction is mainly due to smaller systematic errors at low  $k$  (Fig. 5). This is observed for all spectra.

When using **noSCF** phases and amplitudes, in most cases, the quality factors are slightly larger for **MDV** than for **MDR**. This is due to a lower number of free amplitude parameters to compensate systematic errors. The quality factors ratios  $QF_{\text{MDV}}/QF_{\text{MDR}}$  are close to 1 for all spectra (lower than 1.16), except for OxaliPt-liq3 (1.42).<sup>31</sup> The main difference concerns the  $s_0^2$  values, which plays the role of a scale factor and is highly correlated to  $\sigma_1^2$ . But all distances are identical within the error bars. When using **SCF** phases and amplitudes, the fits obtained for **MDR** and **MDV** can hardly be distinguished, with quality factors ratios lower than 1.04 for all spectra. Thus both **MDR** and **MDV** are good approaches to limit the number of fitted parameters, for both **noSCF** and **SCF** phases and amplitudes.

A systematic test on the performance of the use of DWs in the fitting procedure is given in Table IV, which collects the amplitude parameters ( $s_0^2$  and  $\sigma_1^2$ ) and quality factors for all fits with the **MDR** DWs choice (DWs ratios). Concerning the fitted  $s_0^2$  values, a systematic change is observed. However,

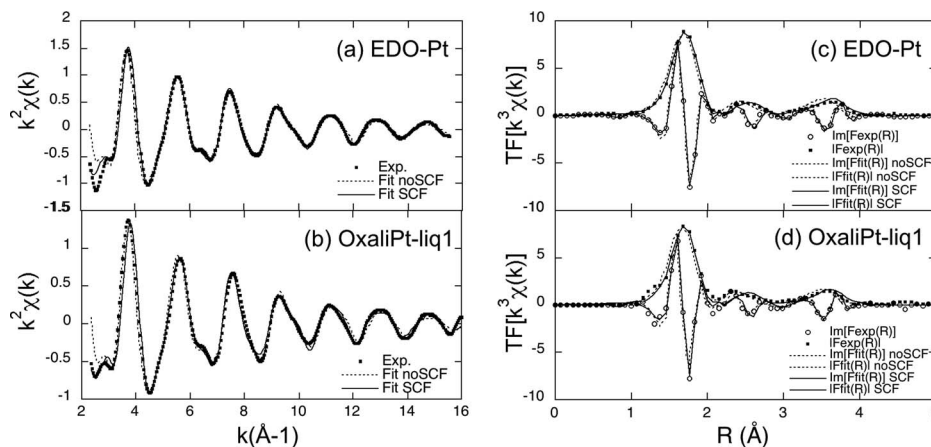
FIG. 5. EXAFS fit of EDO-Pt (a) and (c) and OxaliPt-liq1 (b) and (d) using **MDR**.

TABLE IV.  $s_0^2$ ,  $\sigma_1^2$ , and quality factors issued from the fit of the different spectra, with MDR conditions and FEFF (a) or empirical (b) mean free path.

(a)		noSCF			SCF			CP-MD
$\lambda_{\text{FEFF}}$	$(\varepsilon)$	$s_0^2$	$\sigma_1^2 \times 10^4 (\text{\AA})^2$	QF	$s_0^2$	$\sigma_1^2 \times 10^4 (\text{\AA})^2$	QF	$\sigma_1^2 \times 10^4 (\text{\AA})^2$
EDO-Pt	0.015	1.24(7)	36(5)	1.93	0.95(3)	26(3)	0.65	24
Oxali-liq1	0.015	1.07(6)	32(4)	1.54	0.80(5)	22(4)	1.35	
Oxali-liq2	0.018	1.09(6)	28(4)	0.97	0.81(5)	18(4)	0.93	
Oxali-liq3	0.011	1.05(4)	36(3)	1.18	0.79(4)	27(4)	1.30	
Oxali-sol	0.027	1.10(9)	32(6)	0.76	0.85(4)	23(4)	0.28	
(b)		noSCF			SCF			CP-MD
$\lambda_{\text{emp}}$	$(\varepsilon)$	$s_0^2$	$\sigma_1^2 \times 10^4 (\text{\AA})^2$	QF	$s_0^2$	$\sigma_1^2 \times 10^4 (\text{\AA})^2$	QF	$\sigma_1^2 \times 10^4 (\text{\AA})^2$
EDO-Pt	0.015	1.22(7)	44(6)	2.00	0.82(4)	27(4)	1.30	24
Oxali-liq1	0.015	1.05(7)	39(6)	1.70	0.69(5)	23(5)	1.61	
Oxali-liq2	0.018	1.06(6)	33(4)	1.11	0.70(5)	18(5)	1.17	
Oxali-liq3	0.011	1.03(6)	43(5)	1.51	0.68(4)	27(4)	1.85	
Oxali-sol	0.027	1.06(9)	38(7)	0.86	0.73(5)	24(5)	0.38	

under the same amplitude, phase and mean free paths conditions,  $s_0^2$  values for the four experimental spectra are equal within the error bars. Thus, the observed significant variations are due to well-defined systematic factors: (i) theoretical simulation or experimental spectra, (ii) **SCF** or **noSCF** phases and amplitudes, and (iii) FEFF or empirical mean free path. The difference between EDO-Pt simulated spectrum on the one hand and oxaliplatin experimental spectra on the other one can be easily explained by systematic errors induced by the extraction procedure for the experimental spectra. The two other  $s_0^2$  variation factors are discussed below.

For EDO-Pt simulated spectrum, the comparison between the fitted DWs and DWs issued from the CP-MD trajectory allows us to find out whether the fitting conditions succeed or not in providing the correct DWs values. When using **SCF** phases and amplitudes, the fitted DWs are equal to the MD values, within the error bars ( $\sigma_1^2 = 26(3) \times 10^{-4} \text{\AA}^2$ ). This is also true when introducing systematic errors on the mean free path, by replacing FEFF mean free path (the mean free path used in the simulated spectrum generation, Table IV(a)) by an empirical one, based on the standard minimum curve<sup>13</sup> ( $\Gamma = 0.7$ ,  $\eta = 3.0$  Table IV(b)). With SCF based phases and amplitudes, the  $\sigma_1^2$  values are not affected, the systematic errors on mean free path are compensated by the sole  $s_0^2$  parameter. Thus, using **SCF** phases and amplitudes, it is possible to extract the right  $\sigma_1^2$  value from the EXAFS fit, when fitting both  $s_0^2$  and  $\sigma_1^2$ . When using **noSCF** phases and amplitudes, the  $s_0^2$  and  $\sigma_1^2$  values are more mean free path dependent, and correlations result in an artificial increase of both parameters which do not reflect the actual values (CP-MD) anymore.

A similar behavior of both  $s_0^2$  and  $\sigma_1^2$  is observed for all experimental spectra. Nonreliable  $\sigma_1^2$  values are obtained when using **noSCF** phases and amplitudes, but reasonable values are found when using **SCF** phases and amplitudes, on the basis of the simulated spectrum study. With **SCF**, the  $\sigma_1^2$  values are not affected by the choice of the mean free path model, as for the simulated spectrum. The  $\sigma_1^2$  values range between 18(5) and 27(4)  $\times 10^{-4} \text{\AA}^2$ , with an average value of

$23 \times 10^{-4} \text{\AA}^2$ , in good agreement with the theoretical value,  $24 \times 10^{-4} \text{\AA}^2$ . Thus, the results obtained from the experimental spectra suggest that CP-MD EDO-Pt in solution trajectory gives a good description of the experimental distance distributions for oxaliplatin in solution, at room temperature. A deeper insight into the DW determination would imply to include the temperature dependence, what would lead to a set of new experiments and computer simulations at different temperatures. However, the aim of this study is to improve accurate constrained EXAFS fitting.

### C. Transferability to related compounds

Since the computation of a CP-MD trajectory for every system under XAS study is not practical, it is important to assess to which point these computed DWs are transferable to related compounds. The transferability of EDO-Pt CP-MD DWs has been tested by using both **MDR** and **MDV** strategies for the fit of bis(oxalato) platinate(II) and bis(ethylenediamine) platinum(II). In these compounds, only one of the two oxaliplatin ligands, oxalate or ethylenediamine, is present. Thus, the 7-shell model used for EDO-Pt and oxaliplatin must be adapted: The fit of bis(oxalato) platinate(II) includes six of the seven scattering paths of oxaliplatin, with the

TABLE V. EXAFS fit of bis(oxalato) platinate(II).<sup>a</sup>

	noSCF		SCF		Cryst.
	MDR	MDV	MDR	MDV	
$s_0^2$	1.10(5)	1.06(4)	0.86(4)	0.91(3)	
$\sigma_1^2 \times 10^4$ <sup>b</sup>	27(3)	24	19(3)	24	
$R_1$	1.99(1)	1.99(1)	2.00(1)	2.00(1)	2.00(1)
$R_2$	2.77(1)	2.77(1)	2.79(1)	2.79(1)	2.78(1)
$R_4$	3.97(1)	3.97(1)	4.00(1)	4.01(1)	3.97(2)
QF	1.76	1.74	1.53	1.64	

<sup>a</sup>Experimental error ( $\varepsilon$ ) = 0.012.

<sup>b</sup> $\sigma_1^2$  values expressed in  $\text{\AA}^2$ , distances expressed in  $\text{\AA}$ .  $R_5$ ,  $R_6$ , and  $R_7$  derived from  $R_4$  as described in Sec. II C.

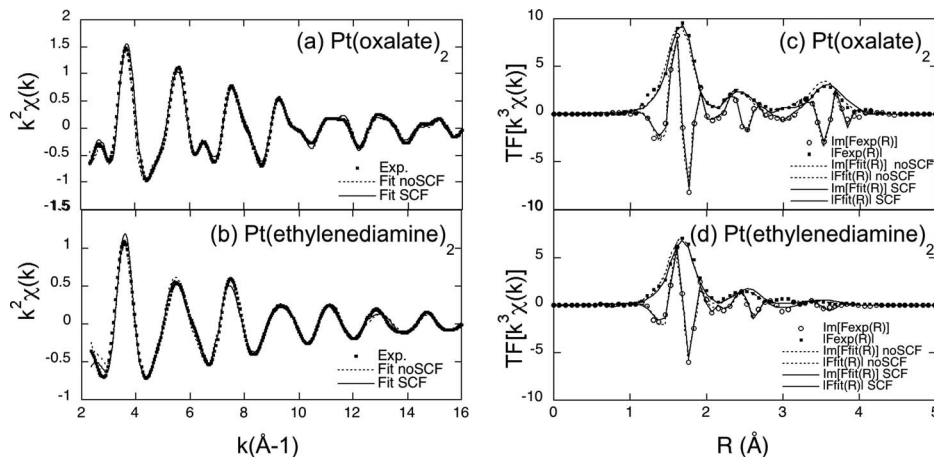


FIG. 6. Fit of bis(oxalato) platinate(II) (a) and (c) and bis(ethylenediamine)platinum(II) (b) and (d) using **MDR**.

constraints described in Sec. II C. Scattering path 3 (Pt-C<sub>ed</sub>) is not included in the model. The fit of bis(ethylenediamine) platinum(II) only includes paths 1 (1st coordination sphere single scattering), 3 (Pt-C<sub>ed</sub> single scattering), and 7 (multiple scattering through platinum). The fitted parameters are presented in Tables V and VI. Figure 6 shows the experimental and fitted EXAFS signals for **MDR**.

For both compounds, the use of Edo-Pt CP-MD based DWs leads to good quality fits. The quality factors are close to one, and the fitted distances are equal to the crystallographic ones,<sup>28</sup> within the error bars. **MDR** and **MDV** strategies give close results. The fits differ only by their  $s_0^2$  and  $\sigma_1^2$  values. Thus, the two approaches present a similar performance in the determination of the effective distances.

When fitting one DW, in the **MDR** strategy, we obtain  $\sigma_1^2$  values slightly lower than the average  $\sigma_1^2$  observed for oxaliplatin. However, taking into account the variability of  $\sigma_1^2$  observed among the different oxaliplatin experimental spectra (Table IV), it is difficult to say how significant is the difference in the  $\sigma_1^2$  values obtained for bis(oxalato) platinate (II) and bis(ethylenediamine) platinum(II).

The main result of this section is that the transferability of EDO-Pt DWs is assessed for structure determination using **MDR** or **MDV** in EXAFS fit, for both **SCF** and **noSCF** phases and amplitudes. In this work, the transferability can be easily applied because we consider closely related complexes. An extension of the method to more different and complex

bioinorganic systems would imply a good knowledge of DWs values, which can be system dependent. However, as soon as it is possible to build a first reasonable structural model, theoretical DWs values can be determined, either by CP-MD or by normal modes analysis, in order to constrain the fit of the whole EXAFS signal.

#### IV. CONCLUDING REMARKS

Extraction of accurate information on the structural disorder in chemical systems from EXAFS fitting is difficult, because of correlations between amplitude parameters, and systematic errors affecting these amplitudes. This study has shown that when working with simulated EXAFS spectra, most sources of these systematic errors can be cancelled out. This makes possible to assess the ability of EXAFS fitting to recover information on DWs, and then to apply the information gained on simulated spectra to experimental ones. The case studied has been based on the use of a CP-MD simulation of a good spectroscopical model of oxaliplatin in water, EDO-Pt, that provided:

- (i) a good knowledge of EDO-Pt configurational space, average distances, and distance distributions, including eventual anharmonicity;
- (ii) the generation of average simulated spectra, which reflect the actual static and dynamic disorder, with the aid of well-tested *ab initio* XAS codes, and that could be fitted as experimental ones;
- (iii) the precise knowledge of parameters affecting the photoelectron behavior, in terms of potentials, scattering paths phases and amplitudes, reduction factor and mean free path, since the average spectra are simulated;
- (iv) and, thus, the opportunity to check the impact of eventual systematic errors on these parameters.

It is not possible to fulfill all these points on the sole basis of experimental spectra.

Distance distributions issued from the CP-MD trajectory showed a negligible anharmonicity, for all significant scattering paths associated to the Pt complex. Thus, the estimation of DWs as the second cumulant is reliable. The CP-MD DWs

TABLE VI. EXAFS fit of bis(ethylenediamine) platinum(II).<sup>a</sup>

	noSCF		SCF		Cryst.
	MDR	MDV	MDR	MDV	
$s_0^2$	0.89(5)	0.84(4)	0.73(3)	0.78(3)	
$\sigma_1^2 \times 10^4$ <sup>b</sup>	29(4)	24	17(3)	24	
$R_1$	2.01(1)	2.01(1)	2.04(1)	2.04(1)	2.04(1)
$R_3$	2.89(1)	2.89(1)	2.91(1)	2.91(1)	2.89(1)
$R_7$	4.05(5)	4.05(5)	4.15(3)	4.15(3)	4.09(1)
QF	0.32	0.33	0.22	0.26	

<sup>a</sup>Experimental error ( $\epsilon$ ) = 0.023.

<sup>b</sup> $\sigma_1^2$  values expressed in Å<sup>2</sup>, distances expressed in Å.

values were successfully used for the fit of oxaliplatin experimental spectra, in two different approaches: using the CP-MD DWs absolute values, or fitting a DW for one path and applying the theoretical DW ratios. The two approaches give satisfactory results, from both the structural point of view and the fit quality point of view.

Use of DWs ratios on simulated spectra showed that EXAFS fitting could supply DWs information, provided that phases and amplitudes were calculated by the self-consistent-field approach. This result is not affected by the choice of the mean free path model: the impact of error on this parameter is corrected by a scale factor. Fit under the same conditions of oxaliplatin experimental spectra showed that CP-MD gives a good representation of the DWs for oxaliplatin in solution.

Fitting  $s_0^2$  was necessary in our study in order to check that the  $\sigma_1^2$  values were not affected by the other amplitude parameters discussed in this paper. However, it is worth underlining that it is not a standard recommended procedure, because of correlations. When fitting unknown compounds spectra,  $s_0^2$  should be fixed at the value obtained from a model compound.

EDO-Pt CP-MD based DWs were useful for the fit of bis(oxalato) platinate(II) and bis(ethylenediamine) platinum(II), in both approaches, MD values or ratios, even with a standard approach for phases and amplitudes. The transferability is assessed for all relevant scattering paths, including multiple scattering paths through platinum. Thus, even if the use of the DWs values presented in this paper is limited to specific systems, we believe that the strategy of including theoretical DWs ratios to constrain the fits is a potentially useful procedure what deserves further development.

## ACKNOWLEDGMENTS

We would like to thank Dr. Jacques Moscovici, Dr. Luca Olivi, Professor Gilberto Vlaic, Professor Adela Muñoz-Paez, and Dr. Stéphanie Belin for their contribution to data collection at ELETTRA, ESRF, and SOLEIL. We would also thank Professor Christophe Den Auwer for useful discussions. The European Community Research Infrastructure Action under the FP6 Structuring the European Research Area Program (through the Integrated Infrastructure Initiative integrating Activity on Synchrotron and Free Electron Laser Science) and the Spanish Ministerio de Ciencia e Innovación (CTQ2011-25932) are gratefully acknowledged for financial support. E.C.B. acknowledges Junta de Andalucía for a post-doctoral fellowship (P06-FQM-01484). We also acknowledge the University of Paris - East Creteil which funded part of this work by providing a visiting professor position to Professor Enrique Sanchez Marcos.

<sup>1</sup>D. E. Sayers, E. A. Stern, and F. W. Lytle, *Phys. Rev. Lett.* **27**, 1204 (1971).

<sup>2</sup>J. F. Lee, P. H. Citrin, P. Eisenberger, and B. M. Kincaid, *Rev. Mod. Phys.* **53**(4), 769 (1981); M. Newville, B. Ravel, D. Haskel, J. J. Rehr, E. A. Stern, and Y. Yacoby, *Physica B* **208–209**, 154 (1995); *Introduction to XAFS*, edited by G. Bunker (Cambridge University Press, New York, 2010).

<sup>3</sup>K. Provost, E. C. Beret, D. Muller, E. Sanchez Marcos, and A. Michalowicz, "Impact of the number of fitted Debye Wallers on EXAFS fitting," *J. Phys.: Conf. Ser.* (in press).

<sup>4</sup>P. W. Loeffen and R. F. Pettifer, *Phys. Rev. Lett.* **76**, 636 (1996).

<sup>5</sup>T. Yokoyama, K. Kobayashi, T. Ohta, and A. Ugawa, *Phys. Rev. B* **53**, 6111 (1996); T. Yokoyama, T. Ohta, and H. Sato, *ibid.* **55**, 11320 (1997).

<sup>6</sup>N. Dimakis and G. Bunker, *Phys. Rev. B* **70**, 195114 (2004); N. Dimakis, T. Mion, and G. Bunker, *J. Phys.: Conf. Ser.* **190**, 012011 (2009); N. Dimakis, T. Mion, C. Ramirez, and G. Bunker, *ibid.* **190**, 012198 (2009); A. V. Poiarkova and J. J. Rehr, *Phys. Rev. B* **59**, 948 (1999); F. D. Vila, J. J. Rehr, H. H. Rossner, and H. J. Krappe, *ibid.* **76**, 014301 (2007).

<sup>7</sup>A. Filipponi, P. D'Angelo, N. V. Pavel, and A. Di Cicco, *Chem. Phys. Lett.* **225**, 150 (1994).

<sup>8</sup>B. J. Palmer, D. M. Pfund, and J. L. Fulton, *J. Phys. Chem.* **100**, 13393 (1996); L. Campbell, J. J. Rehr, G. K. Schenter, M. I. McCarthy, and D. Dixon, *J. Synchrotron Radiat.* **6**, 310 (1999); F. Jalilehvand, D. Spångberg, P. Lindqvist-Reis, K. Hermansson, I. Persson, and M. Sandström, *J. Am. Chem. Soc.* **123**(3), 431 (2001).

<sup>9</sup>P. J. Merklings, A. Muñoz-Paez, J. M. Martínez, R. R. Pappalardo, and E. Sánchez Marcos, *Phys. Rev. B* **64**, 012201 (2001).

<sup>10</sup>P. J. Merklings, A. Muñoz-Paez, and E. Sánchez Marcos, *J. Am. Chem. Soc.* **124**, 10911 (2002).

<sup>11</sup>Y. W. Hsiao, Y. Tao, J. E. Shokes, R. A. Scott, and U. Ryde, *Phys. Rev. B* **74**(21), 214101 (2006).

<sup>12</sup>B. K. Teo and P. A. Lee, *J. Am. Chem. Soc.* **101** (11), 2815 (1979); J. J. Rehr, J. J. Kas, M. P. Prange, A. P. Sorini, Y. Takimoto, and F. Vila, *C. R. Phys.* **10**(2009), 548 (2009); J. J. Rehr and R. C. Albers, *Rev. Mod. Phys.* **72**, 621 (2000); S. Tomic, B. G. Searle, A. Wander, N. M. Harrison, A. J. Dent, J. F. W. Mosselmanns, and J. E. Inglesfield, CCLRC Technical Report DL-TR-2005-001, ISSN, 1362 (2005); A. Di Cicco, *GNXAS, Extended Suite of Programs for Advanced X-ray Absorption Data Analysis: Methodology and Practice* (Task, Gdansk, Poland, 2009); S. D. Kelly and B. Ravel, *AIP Conf. Proc.* **882**, 135 (2007).

<sup>13</sup>B. K. Teo, in *EXAFS: Basic Principles and Data Analysis (Inorganic Chemistry Concepts)* (Springer-Verlag, Berlin, 1986), Vol. 9.

<sup>14</sup>J. J. Rehr, R. C. Albers, and S. I. Zabinsky, *Phys. Rev. Lett.* **69**(23), 3397 (1992); J. J. Kas, A. P. Sorini, M. P. Prange, L. W. Cambell, J. A. Soininen, and J. J. Rehr, *Phys. Rev. B* **76**, 195116 (2007); M. Newville, J. J. Kas, and J. J. Rehr, *J. Phys.: Conf. Ser.* **190**, 012023 (2009).

<sup>15</sup>J. Graham, M. Muhsin, and P. Kirkpatrick, *Nat. Rev. Drug Discovery* **3**(1), 11 (2004); C. Voland, A. Bord, A. Peleraux, G. Penarier, D. Carriere, S. Galieue, E. Cvitkovic, O. Jbilo, and P. Casellas, *Mol. Cancer Ther.* **5**(9), 2149 (2006); L. Kelland, *Nat. Rev. Cancer* **7**(8), 573 (2007); C. Avendano and J. C. Menendez, *Medicinal Chemistry of Anticancer Drugs* (Elsevier, 2008).

<sup>16</sup>A. Ghezzi, M. Aceto, C. Cassino, E. Gabano, and D. Osella, *J. Inorg. Biochem.* **98**(1), 73 (2004); B. A. Woynarowska and J. M. Woynarowski, *BBA-Mol. Basis Dis.* **1587**(2-3), 309 (2002); A. M. Di Francesco, A. Ruggiero, and R. Riccardi, *Cell. Mol. Life Sci.* **59**(11), 1914 (2002); J. Kas-parkova, M. Vojtiskova, G. Natile, and V. Brabec, *Chem.-Eur. J.* **14**(4), 1330 (2008).

<sup>17</sup>N. Summa, W. Schiessl, R. Puchta, N. van Eikema Hommes, and R. van Eldik, *Inorg. Chem.* **45**(7), 2948 (2006).

<sup>18</sup>N. Summa, T. Soldatovic, L. Dahlenburg, Z. D. Bugarcic, and R. van Eldik, *J. Biol. Inorg. Chem.* **12**(4), 461 (2007).

<sup>19</sup>E. Curis, K. Provost, D. Bouvet, I. Nicolis, S. Crauste-Manciet, D. Brossard, and S. Bénazeth, *J. Synchrotron Radiat.* **8**, 716 (2001); D. Bouvet, A. Michalowicz, S. Crauste-Manciet, E. Curis, I. Nicolis, D. Brossard, and K. Provost, *ibid.* **13**, 477 (2006); D. Bouvet, A. Michalowicz, S. Crauste-Manciet, D. Brossard, and K. Provost, *Inorg. Chem.* **45**, 3393 (2006); K. Provost, D. Bouvet-Muller, S. Crauste-Manciet, J. Moscovici, L. Olivi, G. Vlaic, and A. Michalowicz, *Biochimie* **91**, 1301 (2009); K. Provost, D. Bouvet-Muller, S. Crauste-Manciet, L. Olivi, G. Vlaic, and A. Michalowicz, *J. Phys.: Conf. Ser.* **190**, 012206 (2009).

<sup>20</sup>E. C. Beret, R. R. Pappalardo, D. Marx, and E. Sánchez Marcos, *ChemPhysChem* **10**, 1044 (2009).

<sup>21</sup>E. C. Beret, K. Provost, D. Muller, and E. Sánchez Marcos, *J. Phys. Chem. B* **113**, 12343 (2009).

<sup>22</sup>P. J. Merklings, R. Ayala, J. M. Martínez, R. R. Pappalardo, and E. Sánchez Marcos, *J. Chem. Phys.* **119**, 6647 (2003).

<sup>23</sup>A. L. Ankudinov, B. Ravel, J. J. Rehr, and S. D. Conradson, *Phys. Rev. B* **58** (12), 7565 (1998); A. L. Ankudinov, C. E. Bouldin, J. J. Rehr, J. Sims, and H. Hung, *ibid.* **65**, 104107 (2002).

<sup>24</sup>F. Carrera, F. Torrico, D. T. Richens, A. Muñoz-Paez, J. M. Martínez, R. R. Pappalardo, and E. Sanchez Marcos, *J. Phys. Chem. B* **111**, 8223 (2007);

- R. Ayala, J. M. Martinez, R. R. Pappalardo, A. Munoz-Paez, and E. Sanchez Marcos, *Mol. Simul.* **32**, 1035 (2006).
- <sup>25</sup>D. C. Koenigsberger and R. Prins, *X-ray Absorption Principles, Applications, Techniques of EXAFS, SEXAFS, and XANES* (Wiley, New York, 1988); F. W. Lytle, D. E. Sayers, and E. A. Stern, *Physica B* **158**, 701 (1989).
- <sup>26</sup>A. Michalowicz, J. Moscovici, D. Bouvet-Muller, and K. Provost, *J. Phys.: Conf. Ser.* **190**, 012034 (2009).
- <sup>27</sup>M. A. Bruck, R. Bau, M. Noji, K. Inagaki, and Y. Kidani, *Inorg. Chim. Acta* **92** (4), 279 (1984).
- <sup>28</sup>R. von Mattes and K. Krogmann, *Z. Anorg. Allg. Chem.* **332**, 247 (1964); S. Sato, M. Haruki, and S. Kurita, *Acta Cryst. C* **C46**, 1107 (1990).
- <sup>29</sup>Standard and Criteria in XAFS committee error report, IXS (2000), [ixs.iit.edu/subcommittee\\_reports/sc/err-rep.pdf](http://ixs.iit.edu/subcommittee_reports/sc/err-rep.pdf).
- <sup>30</sup>G. Vlaic, D. Andreatta, A. Cepparo, P. E. Colavita, E. Fonda, and A. Michalowicz, *J. Synchrotron Radiat.* **6**, 225 (1999).
- <sup>31</sup>See supplementary material at <http://dx.doi.org/10.1063/1.4790516> for parameters obtained in the EXAFS fit of the different oxaliplatin spectra, not explicitly presented in this paper.